
Discover Generics
Cost-Effective CT & MRI Contrast Agents
FRESENIUS KABI
WATCH VIDEO

AJNR

# Utility of Percentage Signal Recovery and Baseline Signal in DSC-MRI Optimized for Relative CBV Measurement for Differentiating Glioblastoma, Lymphoma, Metastasis, and Meningioma

M.D. Lee, G.L. Baird, L.C. Bell, C.C. Quarles and J.L. Boxerman

This information is current as of June 19, 2025.

*AJNR Am J Neuroradiol* 2019, 40 (9) 1445-1450
doi: https://doi.org/10.3174/ajnr.A6153
http://www.ajnr.org/content/40/9/1445

# Utility of Percentage Signal Recovery and Baseline Signal in DSC-MRI Optimized for Relative CBV Measurement for Differentiating Glioblastoma, Lymphoma, Metastasis, and Meningioma

M.D. Lee, G.L. Baird, L.C. Bell, C.C. Quarles, and J.L. Boxerman

## ABSTRACT

**BACKGROUND AND PURPOSE:** The percentage signal recovery in non-leakage-corrected (no preload, high flip angle, intermediate TE) DSC-MR imaging is known to differ significantly for glioblastoma, metastasis, and primary CNS lymphoma. Because the percentage signal recovery is influenced by preload and pulse sequence parameters, we investigated whether the percentage signal recovery can still differentiate these common contrast-enhancing neoplasms using a DSC-MR imaging protocol designed for relative CBV accuracy (preload, intermediate flip angle, low TE).

**MATERIALS AND METHODS:** We retrospectively analyzed DSC-MR imaging of treatment-naïve, pathology-proved glioblastomas ($n$ = 14), primary central nervous system lymphomas ($n$ = 7), metastases ($n$ = 20), and meningiomas ($n$ = 13) using a protocol designed for relative CBV accuracy (a one-quarter-dose preload and single-dose bolus of gadobutrol, TR/TE = 1290/40 ms, flip angle = 60° at 1.5T). Mean percentage signal recovery, relative CBV, and normalized baseline signal intensity were compared within contrast-enhancing lesion volumes. Classification accuracy was determined by receiver operating characteristic analysis.

**RESULTS:** Relative CBV best differentiated meningioma from glioblastoma and from metastasis with areas under the curve of 0.84 and 0.82, respectively. The percentage signal recovery best differentiated primary central nervous system lymphoma from metastasis with an area under the curve of 0.81. Relative CBV and percentage signal recovery were similar in differentiating primary central nervous system lymphoma from glioblastoma and from meningioma. Although neither relative CBV nor percentage signal recovery differentiated glioblastoma from metastasis, mean normalized baseline signal intensity achieved 86% sensitivity and 50% specificity.

**CONCLUSIONS:** Similar to results for non-preload-based DSC-MR imaging, percentage signal recovery for one-quarter-dose preload-based, intermediate flip angle DSC-MR imaging differentiates most pair-wise comparisons of glioblastoma, metastasis, primary central nervous system lymphoma, and meningioma, except for glioblastoma versus metastasis. Differences in normalized post-preload baseline signal for glioblastoma and metastasis, reflecting a snapshot of dynamic contrast enhancement, may motivate the use of single-dose multiecho protocols permitting simultaneous quantification of DSC-MR imaging and dynamic contrast-enhanced MR imaging parameters.

**ABBREVIATIONS:** DCE = dynamic contrast-enhanced; FA = flip angle; NAWM = normal-appearing white matter; PCNSL = primary central nervous system lymphoma; PSR = percentage signal recovery; rCBV = relative cerebral blood volume; SI = signal intensity; AUC = area under the curve

Conventional MR imaging cannot always differentiate contrast-enhancing malignant brain tumors, including glioblastoma, primary central nervous system lymphoma (PCNSL), and cerebral metastasis.[1] Meningioma and dural-based metastasis may also appear similar on conventional MR imaging. Because management differs for these tumors, timely and accurate identification is imperative. Perfusion-weighted MR imaging can help characterize brain tumors, and DSC-MR imaging is the most popular method for measuring brain perfusion with MR imaging.[2] By tracking T2*-weighted signal changes during the first passage of a gadolinium-based contrast agent bolus, relative cerebral blood volume (rCBV) compared with normal-appearing white matter (NAWM) and percentage signal recovery (PSR) compared with baseline can be calculated.[3] rCBV reflects tumor neoangiogenesis

Received March 6, 2019; accepted after revision June 21.

From the Warren Alpert Medical School of Brown University (M.D.L., J.L.B.), Providence, Rhode Island; Department of Diagnostic Imaging (G.L.B., J.L.B.), Rhode Island Hospital, Providence, Rhode Island; and Division of Neuroimaging Research (L.C.B., C.C.Q.), Barrow Neurological Institute, Phoenix, Arizona.

This work was supported by the National Institutes of Health/National Cancer Institute, CA158079-01 (C. Chad Quarles and Laura C. Bell).

Paper previously presented, in part, as an oral scientific presentation (O-35) at: Annual Meeting of the American Society of Neuroradiology and the Foundation of the ASNR Symposium, June 2–7, 2018; Vancouver, British Columbia, Canada.

Please address correspondence to Jerrold L. Boxerman, MD, PhD, FACR, Rhode Island Hospital, Department of Diagnostic Imaging, 593 Eddy St, Providence, RI 02903; e-mail: jboxerman@lifespan.org

Indicates open access to non-subscribers at www.ajnr.org

http://dx.doi.org/10.3174/ajnr.A6153

and correlates with glioma grade.[4] The PSR reflects a complex interplay of capillary permeability related to blood-brain barrier integrity and contrast agent extravasation from tumor capillaries, as well as tumor cell size and cell density.[5]

Because glioblastoma and lymphoma have a disrupted BBB, which is absent in metastases and meningiomas, gadolinium-based contrast agent extravasates in these tumors, inducing T1 and T2* shortening that obfuscates rCBV measurements. Preload contrast agent administration helps mitigate these leakage effects, rendering rCBV measurements more accurate.[6,7] However, the introduction of a preload dose impacts PSR measurements, because Bell et al[8] demonstrated that PSR in high-grade gliomas decreases with increasing preload dose. Likewise, Boxerman et al[9] demonstrated that while T1-sensitive DSC-MR imaging acquisitions with a high flip angle (FA) and short-TE yield increased PSR in high-grade gliomas, preload administration diminishes the variation in PSR measured with different protocols. Therefore, a trade-off exists for DSC-MR imaging acquisition parameters between PSR sensitivity and rCBV accuracy. PSR has been shown to significantly differ among glioblastoma, PCNSL, and metastasis when using a non-leakage-corrected protocol optimized for PSR sensitivity with a high FA, intermediate TE, and without preload at 1.5T.[10] However, DSC-MR imaging performed for rCBV measurement often includes a preload dose of contrast to minimize contrast agent leakage effects.[7] This study aimed to determine whether the PSR can still differentiate these common contrast-enhancing brain tumors using a preload-based, intermediate-FA, low-TE DSC-MR imaging protocol designed for rCBV accuracy.[2,6]

## MATERIALS AND METHODS

### Patients

The institutional review board approved this Health Insurance Portability and Accountability Act–compliant study, and informed consent was waived. We retrospectively queried the neuropathology data base at Rhode Island Hospital for patients with treatment-naïve, biopsy-proved cerebral glioblastoma, metastasis, lymphoma, or meningioma who underwent preoperative DSC-MR imaging with identical field strength and pulse sequence parameters between January 2015 and September 2017. We identified 54 patients: 14 with glioblastomas (9 men; mean age, 62.4 years; range, 47–78 years), 7 with PCNSL (5 men; mean age, 65.9 years; range, 47–82 years), 13 with meningiomas (2 men; mean age, 65.8 years; range, 38–82 years), and 20 with metastases (7 men; mean age, 59.4 years; range, 29–82 years; 12 lung, 2 breast, 2 colon, 2 melanoma, 1 osteosarcoma, 1 ovarian primary).

### Image Acquisition

All DSC-MR imaging (gradient-echo EPI: TR = 1290 ms, TE = 40 ms, FA = 60°, matrix size = 128 × 128, slice thickness = 5 mm) was performed at 1.5T (Magnetom Aera; Siemens, Erlangen, Germany) with identical 16-channel head coils. Before image acquisition, a one-quarter-dose (0.025 mL/kg) gadobutrol (Gadavist; Bayer Schering Pharma, Berlin, Germany) preload dose was administered (5 mL/s). After 40–50 baseline acquisitions, a single-dose (0.1 mL/kg) gadobutrol bolus was injected (5 mL/s) and imaging continued for a total of 120 baseline-plus-postbolus image acquisitions (~2.5 minutes). Following DSC-MR imaging, postcontrast spin-echo T1-weighted images (TR = 400 ms, TE = 17 ms, FA = 90°, slice thickness = 5 mm, matrix = 256 × 256, NEX = 1) were acquired at slice positions and orientations identical to those of the DSC-MR imaging to simplify segmentation.

### Image Postprocessing

A neuroradiologist with 15 years' post-Certificate of Added Qualification experience semiautomatically segmented contrast-enhancing lesion volumes on postcontrast T1-weighted images using the IB Delta Suite plug-in (Imaging Biometrics, Elm Grove, Wisconsin) for OsiriX-MD (http://www.osirix-viewer.com), avoiding necrosis and susceptibility artifacts. For normalization, a 70- to 80-mm$^2$ elliptic ROI was placed in the contralateral NAWM. We computed rCBV maps using commercial software (OsiriX Pro Version 2.04 and IB Neuro Version 1.1, Imaging Biometrics) that incorporates a postprocessing leakage-correction algorithm and normalized CBV to mean CBV in NAWM (rCBV).[4,11] Voxels with subzero rCBV were excluded from the final analysis. PSR was calculated for each voxel using the following formula: PSR = $(S_1 - S_{min})/(S_0 - S_{min})$, where $S_0$ is the baseline signal intensity (SI) averaged over the first 10 time points, $S_1$ is the tail averaged over the last 10 time points, and $S_{min}$ is the minimum SI in the dynamic series. PSR maps were generated without postprocessing leakage correction using Matlab and Statistics Toolbox Release 2017b (MathWorks, Natick, Massachusetts). In addition to rCBV and PSR, we also computed the normalized baseline DSC-MR imaging signal as $S_{0,tumor}/S_{0,NAWM}$. To qualitatively compare signal-time curves for the different tumor types, we computed the population-average relative signal-time curves as $S_{tumor}(t)/S_{0,tumor}$ for each of the 4 tumor types.

### Statistical Analysis

All modeling was performed using SAS Software, Version 9.4 (SAS Institute, Cary, North Carolina) with the LOGISTIC and GLIMMIX procedures. Mean and interval estimates were calculated for rCBV, PSR, and normalized baseline signal $S_0$ by tumor pathology using generalized linear modeling, assuming a log-normal distribution. Receiver operating characteristic analysis was performed for each parameter and each pair-wise comparison to calculate the area under the curve (AUC). The Youden Index was used to examine the diagnostic performance of different thresholds, though empiric thresholds should be interpreted with caution.[12] Somers D, a measure of the correlation between variables that are not both continuous (ranging between −1.0 and 1.0 like the Pearson $r$), was calculated to estimate the correlation between measured parameters (rCBV, PSR, $S_0$) and tumor type. All interval estimates were calculated for 95% confidence.

## RESULTS

Mean rCBV, PSR, and normalized baseline SI for each tumor type are summarized in Fig 1. The diagnostic performance of these parameters is summarized in the Table. The average normalized signal-time curves for each tumor type are compared in Fig 2.

As indicated with receiver operating characteristic analysis, rCBV differentiated glioblastoma from PCNSL (AUC, 0.79; 95% CI, 0.58–0.99), and meningioma from glioblastoma (AUC, 0.84;

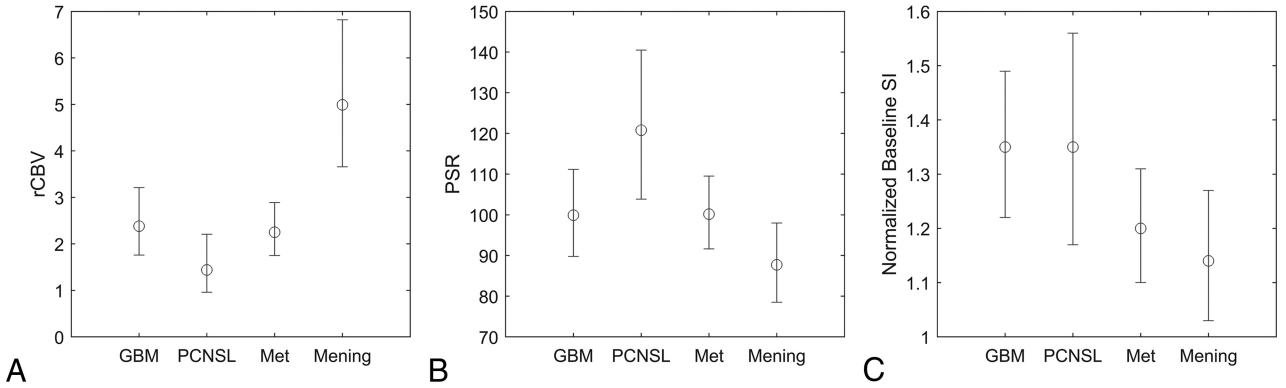


**FIG 1.** Comparisons of rCBV (*A*), PSR (*B*), and normalized baseline SI (*C*) estimates with 95% confidence intervals for glioblastoma, PCNSL, metastasis (Met), and meningioma (Mening).

**Pair-wise discrimination performance (Somers D) of perfusion parameters and baseline SI**

| Pair-wise Comparison | rCBV | PSR | Baseline SI |
|---|---|---|---|
| GBM vs PCNSL | 0.79 (0.58–0.99)<br>D = 0.57 | 0.83 (0.64–1.00)<br>D = 0.65 | 0.50 (0.23–0.77)<br>D = 0.00 |
| GBM vs metastasis | 0.43 (0.24–0.63)<br>D = −0.14 | 0.49 (0.28–0.69)<br>D = −0.03 | 0.66 (0.47–0.84)<br>D = 0.31 |
| GBM vs meningioma | 0.84 (0.69–0.99)<br>D = 0.68 | 0.69 (0.47–0.91)<br>D = 0.37 | 0.76 (0.56–0.95)<br>D = 0.52 |
| PCNSL vs metastasis | 0.66 (0.43–0.88)<br>D = 0.31 | 0.81 (0.64–0.97)<br>D = 0.61 | 0.66 (0.43–0.88)<br>D = 0.31 |
| PCNSL vs meningioma | 0.97 (0.90–1.00)<br>D = 0.93 | 0.89 (0.74–1.00)<br>D = 0.78 | 0.71 (0.46–0.97)<br>D = 0.43 |
| Metastasis vs meningioma | 0.82 (0.68–0.96)<br>D = 0.64 | 0.65 (0.44–0.87)<br>D = 0.31 | 0.55 (0.35–0.75)<br>D = 0.10 |

**Note:**—GBM indicates glioblastoma multiforme; D, Somers D.
[a] Data are area AUC and 95% CI).

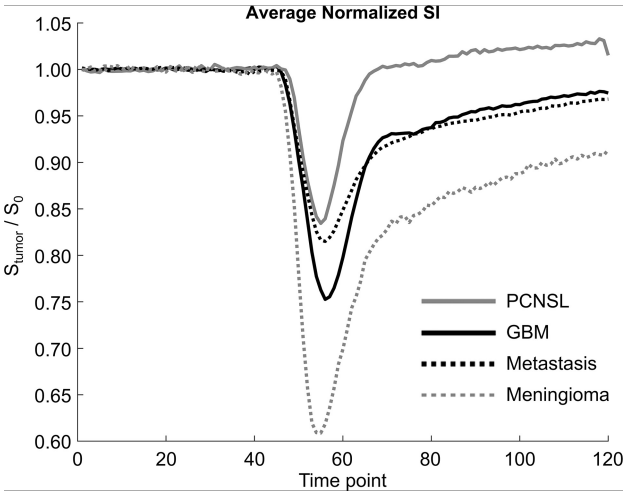


**FIG 2.** Average normalized signal-time curves for glioblastoma multiforme (solid black), PCNSL (solid gray), metastasis (dotted black), and meningioma (dotted gray). TR = 1290 ms, with a total acquisition time of 2 minutes 35 seconds.

95% CI, 0.69–0.99), PCNSL (AUC, 0.97; 95% CI, 0.90–1.00), and metastasis (AUC, 0.82; 95% CI, 0.68–0.96), with more modest differentiation of PCNSL from metastasis (AUC, 0.66; 95% CI, 0.43–0.88). The PSR differentiated PCNSL from glioblastoma (AUC, 0.83; 95% CI, 0.64–1.00), metastasis (AUC, 0.81; 95% CI, 0.64–0.97), and meningioma (AUC, 0.89; 95% CI, 0.74–1.00), with more modest differentiation of glioblastoma from meningioma (AUC, 0.69; 95% CI, 0.47–0.91) and metastasis from meningioma (AUC, 0.65; 95% CI, 0.44–0.87). rCBV was better than PSR in differentiating meningioma from glioblastoma or metastasis. The PSR was better than rCBV in differentiating PCNSL from metastasis. rCBV and PSR performed similarly in differentiating PCNSL from glioblastoma or meningioma.

Glioblastoma and metastasis were poorly differentiated by rCBV (AUC, 0.43; 95% CI, 0.24–0.63) and PSR (AUC, 0.49; 95% CI, 0.28–0.69) but were better distinguished by normalized baseline SI (AUC, 0.66; 95% CI, 0.47–0.84) with an optimal threshold of 1.27 using the Youden index, which achieved 86% sensitivity and 50% specificity.

## DISCUSSION

This study evaluated the utility of PSR for differentiating common contrast-enhancing brain tumors using a DSC-MR imaging protocol designed for rCBV accuracy (preload contrast administration, intermediate FA, low TE).[3] Because treatment of glioblastoma multiforme, brain metastasis, and PCNSL differs substantially, a definitive diagnosis at initial imaging may impact short-term patient management, including subsequent diagnostic tests. Similar to results obtained by Mangla et al[10] for PSR-optimized acquisitions (no preload, high FA, intermediate TE), rCBV-optimized PSR differentiates most pair-wise comparisons of glioblastoma, metastasis, PCNSL, and meningioma. However, our results failed to confirm that PSR is strictly better than rCBV in differentiating tumors. Moreover, neither rCBV nor PSR differentiated glioblastoma and metastasis, which is arguably the most difficult distinction in clinical practice. Thus, our results indicate that rCBV-optimized protocols using preload and parameters with reduced T1 sensitivity may suppress the PSR differences previously demonstrated by PSR-optimized protocols without preload.

Diagnosing PCNSL is important because the first-line treatment for PCNSL is chemotherapy, not surgical resection.[13] We found that, consistent with prior studies,[10,14] PCNSL has lower

rCBV and higher PSR than glioblastoma and metastases; however, we found that the PSR is not strictly better than rCBV at differentiating PCNSL from other types of tumors. While PSR differentiated PCNSL from metastasis better than rCBV, both parameters achieved similar diagnostic performance when differentiating PCNSL from glioblastoma or meningioma. Even with one-quarter-dose preload, PCNSL signal recovery consistently exceeded baseline, similar to studies without preload. PSR > 1 in the setting of elevated rCBV appears to be a particularly simple and effective way to render a prospective, preliminary diagnosis of PCNSL versus other common intra-axial tumors and non-neoplastic pathologies like tumefactive infectious or inflammatory lesions. High PSR exceeding unity is characteristic of PCNSL and reflects the dominance of T1 over T2* effects during the "tail" of the signal-time curve. Although the mechanisms dictating the competition between T1 and T2* effects are complex, tumor vascularity, permeability, cellular features, contrast agent kinetics, pulse sequence parameters, and preload dose all appear to play a role. The unique histologic and physiologic features of PCNSL, such as dense cellularity, small cell size, angiocentric growth pattern, and absence of neoangiogenesis, likely contribute to the characteristically high PSR.[15] By comparison, glioblastoma exhibits greater neoangiogenesis, capillary heterogeneity, and microvascular density.[16] Higher doses of preload may diminish the high PSR of PCNSL, but no studies have evaluated the effect of preload dosing in PCNSL.

We included meningiomas because they can closely resemble dural-based metastases on conventional imaging, and differentiation using DSC-MR imaging would have clinical value. We found that meningiomas have significantly higher rCBV than the other tumors, consistent with a prior case series,[17] primarily owing to the tendency for the meningioma signal-time curve to drop and remain below baseline, resulting in a low PSR. Extra-axial tumors lack a BBB and therefore are expected to have greater contrast extravasation than intra-axial tumors. Contrast-enhancing lesions with an appropriate combination of cell size and density in the absence of a BBB may have postbolus signal-time curves that stay suppressed below the baseline signal, consequently producing artifactually higher rCBV measurements on integration of $\Delta R2^*(t)$. Therefore, it is possible that the reportedly high rCBV for meningioma may reflect low PSR more so than exceptionally high vascular density.

Our study included only intra-axial metastases, and it is unclear whether the rCBV, PSR, and baseline signals of intra-axial metastases are generalizable to dural-based metastases. Extra-axial tumors, for instance, likely have different first-pass kinetics than intra-axial tumors owing to complete absence of the BBB, consequent substantial contrast extravasation and blood pool phase, variable vascularity, and the potential presence of intralesion mineralization. First-pass enhancement may also be more difficult to differentiate from recirculation enhancement in extra-axial tumors. Our results are consistent with 1 study that found significantly higher CBV in 16 meningiomas compared with 6 dural-based metastases,[18] but another study of 12 meningiomas and 8 dural-based metastases found no significant difference in rCBV.[19] Although it is unclear whether preload administration has a substantial impact on CBV estimation in extra-axial lesions given the substantial degree of contrast agent extravasation, neither of these studies used a preload. Whereas the former used a TE (28 ms) and FA (45°) close to currently accepted optimal values for CBV accuracy,[20] the latter did not (8 ms, 7°); this difference could impact CBV estimation. The conclusions of these studies may also differ because of small sample sizes, varying primary tumor types for metastases,[21] and varying grades for meningiomas.[22] We achieved only modest discrimination of metastasis and meningioma using PSR, which was lower for meningiomas than metastases. In light of BBB differences, it is probably best to conclude that if the PSR and CBV of dural-based lesions differ appreciably from those that we found for meningiomas, the lesion is more likely to be a dural-based metastasis. As the signal-time curve becomes more similar to that for meningiomas, with lower PSR and CBV, then the diagnosis is less certain.

Of all pair-wise comparisons, distinguishing a solitary cerebral metastasis from glioblastoma is the most vexing clinical scenario in our experience. We did not observe a significant difference in the rCBV or PSR between glioblastoma and metastasis. These results are consistent with 1 recent study[23] (TE = 80 ms, no preload) but contradict prior no-preload studies (TE = 50 ms, FA = 80°; TE = 54 ms, FA = 35°) that found significantly higher rCBV and PSR in glioblastomas than in metastases.[10,24] Our use of preload and pulse sequence parameters with greater T2* sensitivity appears to have eliminated these PSR differences. While other studies have found that rCBV in peritumoral nonenhancing FLAIR hyperintensity is significantly greater for glioblastoma than metastasis, we restricted our analysis to contrast-enhancing voxels.[10,23]

Although rCBV and PSR could not differentiate glioblastoma from metastasis, we found that glioblastoma exhibits significantly higher normalized baseline signal than metastasis. No previous DSC-MR imaging studies have reported differences in baseline signal after preload administration, to our knowledge. Because baseline signal was measured after preload administration, it provides a snapshot of dynamic contrast-enhanced (DCE)-MR imaging and may serve as a proxy for extravascular extracellular volume ($V_e$) and/or volume transfer constant ($k^{trans}$). Because metastatic capillaries lack a BBB, greater contrast agent extravasation is expected than in glioblastoma, which possesses a BBB, albeit a heterogeneous, disrupted one.[25,26] Greater leakage of contrast agent within metastases should increase its distribution within the extravascular extracellular space, which is more restricted in glioblastomas by densely packed capillary buds composing the microvasculature.[27] Our imaging protocol appears to uncover these differences in contrast agent extravasation after preload administration, though DSC-MR images were not acquired before preload administration, precluding a comparison of baseline signal before any contrast agent administration. Our results are consistent with a prior DCE-MR imaging study reporting higher $k^{trans}$ in glioblastoma versus metastasis[28] and PSR-optimized DSC-MR imaging studies reporting higher PSR in glioblastoma versus metastasis.[10,24,29] Differences in contrast agent leakage are also supported by a DCE-MR imaging study finding that the SI of glioblastoma and melanoma/hypervascular metastasis remained high after contrast agent administration, whereas the signal of nonmelanoma/hypovascular metastasis decreased.[30]

Our results support the pursuit of DCE-MR imaging to differentiate glioblastoma and metastasis. DSC-MR imaging paradigms that perform DCE-MR imaging during the administration of the preload dose[31] or multiecho pulse sequences that acquire DCE-MR imaging data in conjunction with CBV-optimized DSC-MR imaging using a single contrast agent dose[32] may provide the opportunity for comprehensive brain tumor analysis with better differentiation of glioblastoma and metastasis.

In our cohort, PCNSL has greater PSR than glioblastoma but similar baseline signal. This discrepancy may be due to histologic differences affecting the degree to which preload controls T1 leakage effects. The high PSR in PCNSL suggests that the dose of preload used in the present study did not adequately control T1-leakage effects. We expect a preload concentration that fully saturates the extravascular space in PCNSL to result in a lower PSR. Thus, it appears that preload dose-dependent decreases in PSR may differ for different types of tumors.

Further investigation is warranted for determining how to best differentiate brain tumors, especially glioblastoma and metastasis. While guidelines exist, there is no consensus on optimal DSC-MR imaging methodology for brain tumors.[2] Protocol standardization would facilitate comparisons of data among institutions. Given that preload affects PSR, DSC-MR imaging protocols that retain rCBV accuracy without preload may be useful. Such a protocol has recently been shown to provide very accurate rCBV estimates[20] but requires use of a low FA (30°) that would likely suppress PSR differences due to reduced T1-weighting. Multiparametric imaging protocols that combine DCE-MR imaging acquisition during preload administration and DSC-MR imaging offer comprehensive signal morphology analysis and may further characterize and differentiate tumors. Additionally, multiecho DSC-MR imaging protocols have been developed that combine simultaneous gradient-echo acquisitions at different TEs to eliminate T1 effects without preload for accurate rCBV estimation, with a high-FA acquisition providing PSR weighting that may help provide tumor differentiation.[2,32] Single-dose multiecho protocols also enable simultaneous quantification of DCE-MR imaging parameters.[33]

While the discrepancies between the results of our study and those of Mangla et al[10] are most likely due to differences in DSC-MR imaging parameters, there are other methodologic differences that may have impacted our comparisons. Mangla et al included patients who had been treated with steroids and patients with presumed metastatic disease without biopsy. In contrast, all of our cases were treatment-naïve and biopsy-proved, so our analysis is less susceptible to treatment effects and selection bias.

There are several limitations to our study. Because this was a retrospective study, we did not control for the elapsed time between preload administration and the DSC-MR imaging acquisition. However, preload incubation time is unlikely to significantly impact our results because previous studies have shown that the enhancement of gliomas and metastases does not significantly decline during the first 25–30 minutes after contrast injection,[34] and preload incubation times of 5–10 minutes do not affect rCBV estimates in glioblastomas.[6] Our study is also limited by the sample size. Because TR, TE, FA, and field strength all affect baseline signal and PSR, we only analyzed our largest cohort of patients scanned with the same pulse sequence parameters and field strength. We also did not differentiate metastases by primary tumor type, which may be associated with PSR differences.

## CONCLUSIONS

With a protocol designed for rCBV accuracy that incorporates preload and intermediate FA, PSR failed to differentiate glioblastoma from metastasis but could differentiate other pair-wise comparisons of glioblastoma, PCNSL, metastasis, and meningioma. This finding differs from those in previous studies in which PSR-optimized DSC-MR imaging (no preload, high-FA) significantly differentiated glioblastoma and metastasis.[10] However, differences in post-preload baseline signal between glioblastoma and metastasis, reflecting tissue-specific competing T1 and T2* leakage effects, motivate pursuit of DCE-MR imaging and no-preload DSC-MR imaging as tools for differentiating glioblastoma and metastasis. Future directions include assessment of tumor differentiation using PSR obtained with a rCBV-accurate DSC-MR imaging protocol without preload and single-dose multiecho protocols that permit simultaneous quantification of DSC-MR imaging and DCE-MR imaging parameters.

Disclosures: Laura C. Bell—*RELATED*: *Grant*: National Institutes of Health/National Cancer Institute, R01 CA158079.* Christopher C. Quarles—*RELATED*: *Grant*: National Institutes of Health/National Cancer Institute, R01 CA158079.* *Money paid to the institution.

## REFERENCES

1. Stadnik TW, Demaerel P, Luypaert RR, et al. **Imaging tutorial: differential diagnosis of bright lesions on diffusion-weighted MR images.** *Radiographics* 2003;23:e7 Medline
2. Welker K, Boxerman J, Kalnin A, et al; American Society of Functional Neuroradiology MR Perfusion Standards and Practice Subcommittee of the ASFNR Clinical Practice Committee. **ASFNR recommendations for clinical performance of MR dynamic susceptibility contrast perfusion imaging of the brain.** *AJNR Am J Neuroradiol* 2015;36:E41–51 CrossRef Medline
3. Shiroishi MS, Castellazzi G, Boxerman JL, et al. **Principles of T2*-weighted dynamic susceptibility contrast MRI technique in brain tumor imaging.** *J Magn Reson Imaging* 2015;41:296–313 CrossRef Medline
4. Boxerman JL, Schmainda KM, Weisskoff RM. **Relative cerebral blood volume maps corrected for contrast agent extravasation significantly correlate with glioma tumor grade, whereas uncorrected maps do not.** *AJNR Am J Neuroradiol* 2006;27:859–67 Medline
5. Semmineh NB, Xu J, Skinner JT, et al. **Assessing tumor cytoarchitecture using multiecho DSC-MRI derived measures of the transverse relaxivity at tracer equilibrium (TRATE).** *Magn Reson Med* 2015;74:772–84 CrossRef Medline
6. Leu K, Boxerman JL, Ellingson BM. **Effects of MRI protocol parameters, preload injection dose, fractionation strategies, and leakage correction algorithms on the fidelity of dynamic-susceptibility contrast MRI estimates of relative cerebral blood volume in gliomas.** *AJNR Am J Neuroradiol* 2017;38:478–84 CrossRef Medline
7. Boxerman JL, Prah DE, Paulson ES, et al. **The role of preload and leakage correction in gadolinium-based cerebral blood volume estimation determined by comparison with MION as a criterion standard.** *AJNR Am J Neuroradiol* 2012;33:1081–87 CrossRef Medline
8. Bell LC, Hu LS, Stokes AM, et al. **Characterizing the influence of preload dosing on percent signal recovery (PSR) and cerebral blood volume (CBV) measurements in a patient population with high-grade glioma using dynamic susceptibility contrast MRI.** *Tomography* 2017;3:89–95 CrossRef Medline
9. Boxerman JL, Paulson ES, Prah MA, et al. **The effect of pulse se-**

**quence parameters and contrast agent dose on percentage signal recovery in DSC-MRI: implications for clinical applications.** *AJNR Am J Neuroradiol* 2013;34:1364–69 CrossRef Medline

10. Mangla R, Kolar B, Zhu T, et al. **Percentage signal recovery derived from MR dynamic susceptibility contrast imaging is useful to differentiate common enhancing malignant lesions of the brain.** *AJNR Am J Neuroradiol* 2011;32:1004–10 CrossRef Medline
11. Donahue KM, Krouwer HG, Rand SD, et al. **Utility of simultaneously acquired gradient-echo and spin-echo cerebral blood volume and morphology maps in brain tumor patients.** *Magn Reson Med* 2000;43:845–53 CrossRef Medline
12. Altman DG, Royston P. **The cost of dichotomising continuous variables.** *BMJ* 2006;332:1080 Medline
13. Han CH, Batchelor TT. **Diagnosis and management of primary central nervous system lymphoma.** *Cancer* 2017;123:4314–24 CrossRef Medline
14. Xing Z, You RX, Li J, et al. **Differentiation of primary central nervous system lymphomas from high-grade gliomas by rCBV and percentage of signal intensity recovery derived from dynamic susceptibility-weighted contrast-enhanced perfusion MR imaging.** *Clin Neuroradiol* 2014;24:329–36 CrossRef Medline
15. Hartmann M, Heiland S, Harting I, et al. **Distinguishing of primary cerebral lymphoma from high-grade glioma with perfusion-weighted magnetic resonance imaging.** *Neurosci Lett* 2003;338:119–22 CrossRef Medline
16. Liao W, Liu Y, Wang X, et al. **Differentiation of primary central nervous system lymphoma and high-grade glioma with dynamic susceptibility contrast-enhanced perfusion magnetic resonance imaging.** *Acta Radiol* 2009;50:217–25 CrossRef Medline
17. Zimny A, Sasiadek M. **Contribution of perfusion-weighted magnetic resonance imaging in the differentiation of meningiomas and other extra-axial tumors: case reports and literature review.** *J Neurooncol* 2011;103:777–83 CrossRef Medline
18. Kremer S, Grand S, Rémy C, et al. **Contribution of dynamic contrast MR imaging to the differentiation between dural metastasis and meningioma.** *Neuroradiology* 2004;46:642–48 CrossRef Medline
19. Lui YW, Malhotra A, Farinhas JM, et al. **Dynamic perfusion MRI characteristics of dural metastases and meningiomas: a pilot study characterizing the first-pass wash-in phase beyond relative cerebral blood volume.** *AJR Am J Roentgenol* 2011;196:886–90 CrossRef Medline
20. Semmineh NB, Bell LC, Stokes AM, et al. **Optimization of acquisition and analysis methods for clinical dynamic susceptibility contrast MRI using a population-based digital reference object.** *AJNR Am J Neuroradiol* 2018;39:1981–88 CrossRef Medline
21. Kremer S, Grand S, Berger F, et al. **Dynamic contrast-enhanced MRI: differentiating melanoma and renal carcinoma metastases from high-grade astrocytomas and other metastases.** *Neuroradiology* 2003;45:44–49 CrossRef Medline
22. Shi R, Jiang T, Si L, et al. **Correlations of magnetic resonance, perfusion-weighed imaging parameters and microvessel density in meningioma.** *J BUON* 2016;21:709–13 Medline
23. Neska-Matuszewska M, Bladowska J, Sąsiadek M, et al. **Differentiation of glioblastoma multiforme, metastases and primary central nervous system lymphomas using multiparametric perfusion and diffusion MR imaging of a tumor core and a peritumoral zone: searching for a practical approach.** *PLoS One* 2018;13:e0191341 CrossRef Medline
24. Cha S, Lupo JM, Chen M-H, et al. **Differentiation of glioblastoma multiforme and single brain metastasis by peak height and percentage of signal intensity recovery derived from dynamic susceptibility-weighted contrast-enhanced perfusion MR imaging.** *AJNR Am J Neuroradiol* 2007;28:1078–84 CrossRef Medline
25. Long DM. **Capillary ultrastructure in human metastatic brain tumors.** *J Neurosurg* 1979;51:53–58 CrossRef Medline
26. Sarkaria JN, Hu LS, Parney IF, et al. **Is the blood-brain barrier really disrupted in all glioblastomas? A critical assessment of existing clinical data.** *Neuro Oncol* 2018;20:184–91 CrossRef Medline
27. Rojiani AM, Dorovini-Zis K. **Glomeruloid vascular structures in glioblastoma multiforme: an immunohistochemical and ultrastructural study.** *J Neurosurg* 1996;85:1078–84 CrossRef Medline
28. Zhao J, Yang Z, Luo B, et al. **Quantitative evaluation of diffusion and dynamic contrast-enhanced MR in tumor parenchyma and peritumoral area for distinction of brain tumors.** *PLoS One* 2015;10:e0138573 CrossRef Medline
29. Mouthuy N, Cosnard G, Abarca-Quinones J, et al. **Multiparametric magnetic resonance imaging to differentiate high-grade gliomas and brain metastases.** *J Neuroradiol* 2012;39:301–07 CrossRef Medline
30. Jung BC, Arevalo-Perez J, Lyo JK, et al. **Comparison of glioblastomas and brain metastases using dynamic contrast-enhanced perfusion MRI: comparison of glioblastomas and brain.** *J Neuroimaging* 2016;26:240–46 CrossRef Medline
31. Anzalone N, Castellano A, Cadioli M, et al. **Brain gliomas: multicenter standardized assessment of dynamic contrast-enhanced and dynamic susceptibility contrast MR images.** *Radiology* 2018;287:933–43 CrossRef Medline
32. Stokes AM, Skinner JT, Yankeelov T, et al. **Assessment of a simplified spin and gradient echo (sSAGE) approach for human brain tumor perfusion imaging.** *Magn Reson Imaging* 2016;34:1248–55 CrossRef Medline
33. Quarles CC, Gore JC, Xu L, et al. **Comparison of dual-echo DSC-MRI- and DCE-MRI-derived contrast agent kinetic parameters.** *Magn Reson Imaging* 2012;30:944–53 CrossRef Medline
34. Akeson P, Nordström CH, Holtås S. **Time-dependency in brain lesion enhancement with gadodiamide injection.** *Acta Radiol* 1997;38:19–24 Medline